Optimal Control of a Laboratory DC Servo Motor

Przemysław Gorczyca, Krystyn Hajduk, Krzysztof Kołek

AGH University of Science and Technology, Department of Automatics

Abstract: Position control of DC motor is discussed and two control problems are investigated: first, time optimal and second, optimal in the sense of a quadratic performance index. Simple mathematical models, linear and nonlinear, of the DC motor are introduced. In the presented approach, the nonlinear model contains only the nonlinearity of static characteristic. Controllers based on linear and nonlinear models are constructed for both control problems. For the nonlinear model optimal solutions are computed with the use of the MSE method. Comparison of results of real-time and simulation experiments are presented.

Keywords: optimal control, DC servo, MSE method, time optimal control

1. Introduction

A simple laboratory actuator based on DC motor will be investigated. Fig. 1 shows a block diagram of the actuator unit. The DC motor drives a shaft loaded with an inertia disk and then, by a gearbox, an output shaft connected with an output disk. The angle of rotation of the output disk is measured using an incremental encoder. A tachogenerator produces voltage proportional to the angular velocity.
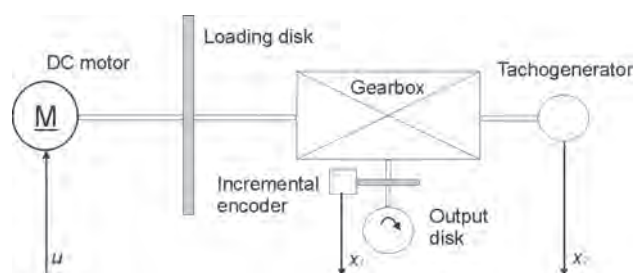

Fig. 1. Actuator unit
Rys. 1. Serwomechanizm

The servomechanism is connected to a computer where a control algorithm is realized based on measurements of angle and angular velocity. The armature voltage is the control signal for the DC motor. Since this voltage is subject to saturation caused by an amplifier, the control signal takes values from the range ±8 V. The measurement system contains an I/O acquisition board equipped with a D/A converter and an A/D converter. The system has no inner feedback for dead zone compensation. The accuracy of measurement of velocity is 5 % while the accuracy of angle measurement is 0,1 %. The minimum sample time is equal to 0,01 s and this value is applied in all experiments.

Position control using the DC motor actuator will be discussed. In the beginning, a simple linear model of the servomechanism is shown and next, a nonlinear model is proposed. Both models are used to design time-optimal control. A time-suboptimal controller with reduced chattering is also constructed. The performance of the time-optimal and suboptimal control is studied in real-time experiments. The remaining part of the chapter is devoted to optimal and suboptimal control, in the sense of a quadratic performance index. First, an optimal linear-quadratic controller is applied to the real system with control saturation. The performance of this suboptimal control is compared with the optimal solution calculated with the nonlinear effects and control bounds taken into account. All real-time experiments are performed in the MATLAB environment using the RTW and RTWT toolboxes [5].

2. Mathematical Models

2.1. Linear Model of DC Motor

A DC motor is described by two classical equations: electrical [1]

$$v(t) = R\,i(t) + K_e\omega(t)$$

and mechanical

$$J\dot\omega(t) = K_m\,i(t) - \beta\omega(t)$$

where $v(t)$ is the input voltage, $i(t)$ is the armature current, $\omega(t)$ is the angular velocity of the rotor, R is the resistance of armature winding, J is the moment of inertia of the moving parts, β is the damping coefficient due to viscous friction, $K_e\omega(t)$ is the EMF, and $K_m\,i(t)$ is the electromechanical torque. Time t is the independent variable. The model is linear because static and dry kinetic friction, as well as saturation are neglected. By combining the electrical and mechanical equations we obtain the equation of a first order inertial system

$$T_s\dot\omega(t) = -\omega(t) + K_s v(t)$$

where the time constant T_s and gain K_s are given by

$$T_s = \frac{RJ}{\beta R + K_e K_m}\,, \qquad K_s = \frac{K_m}{\beta R + K_e K_m}\,.$$

The input voltage is bounded: $-v_{\max} \le v(t) \le v_{\max}$.

The model can be written in a state space notation. Let $x = \mathrm{col}(x_1, x_2)$ be the state vector where x_1 is the angle (in [rad]) determining the position of the output disk, and $x_2 = \omega/n$ is the respective angular velocity (in [rad/s]), where n is the gear ratio. Time t is measured in [s].

The dimensionless control signal is the scaled input voltage, $u(t) = v(t)/v_{max}$. The admissible controls satisfy

$$|u(t)| \leq 1 . \tag{1}$$

The state equations read

$$\dot{x}_1 = x_2 \tag{2}$$

$$\dot{x}_2 = ax_2 + bu \tag{3}$$

where $\quad a = -\dfrac{1}{T_s} < 0, \quad b = \dfrac{v_{max} n K_s}{T_s} > 0 .$

The initial state is given, $x(0) = x^0$. The parameters have the values $T_s = 1,3\,\text{s}$, $n = 30$, $K_s = 0,016\,\text{rad}/(\text{Vs})$, $v_{max} = 8\,\text{V}$ which gives $a = -0,7692\,\text{s}^{-2}$, and $b = 2,954\,\text{rad}/\text{s}^2$.

2.2. Nonlinear Model of DC Motor

In most cases small signal changes are presupposed for the design of control algorithms, so that the control system might be considered linear. In some applications however, nonlinearities in the control loop have to be taken into account. We will use a nonlinear model of the DC motor in the form

$$\dot{x}_1 = x_2 \tag{4}$$

$$\dot{x}_2 = c(u - g(x_2)) \tag{5}$$

where the state variables x_1, x_2 and control u are defined as in the linear model.

The function g is an analytical approximation of the inverted steady state characteristic of the system, which has been determined experimentally. The original inverted characteristic (see Fig. 2) is obtained from measurements. The results of measurements undergo a preliminary treatment consisting of scaling (to express them in appropriate units) and a shift (to remove the bias). An interesting property of the characteristic is that it is discontinuous at zero and shows distinct effects of dry friction in a vicinity of the ori-
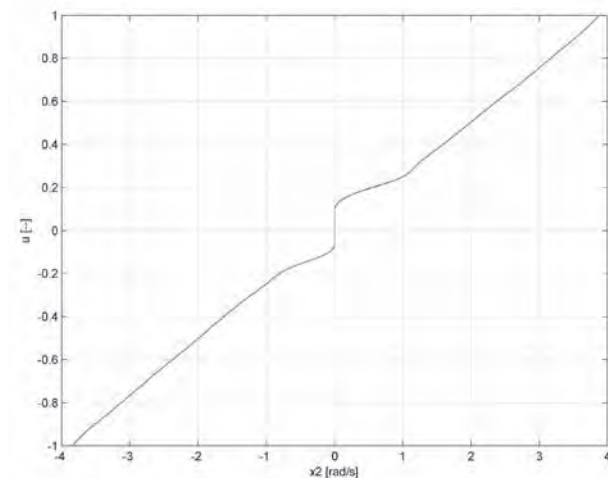

Fig. 2. Inverted steady state characteristic u = g (x2)
Rys. 2. Odwrotna charakterystyka statyczna u = g (x2)

gin. At both ends of the plot (that is, in the regions where the absolute values of the characteristic approach one), slight saturation effects are visible.

It is assumed that g has the form

$$g(x_2) = a_1^- x_2 +$$

$$+\left(a_2^- + a_3^- x_2 + a_4^- x_2^2 + a_5^- x_2^3 + a_6^- x_2^4 \right) \exp(a_7^- x_2) +$$

$$+\left(a_8^- + a_9^- x_2 + a_{10}^- x_2^2 + a_{11}^- x_2^3 \right) \exp(a_{12}^- x_2) , \quad x_2 < 0 \tag{6}$$

$$g(0) = 0 \tag{7}$$

$$g(x_2) = a_1^+ x_2 + \left(a_2^+ + a_3^+ x_2 + a_4^+ x_2^2 + a_5^+ x_2^3 \right) \exp(a_6^+ x_2) +$$

$$+\left(a_7^+ + a_8^+ x_2 + a_9^+ x_2^2 + a_{10}^+ x_2^3 \right) \exp(a_{11}^+ x_2) , \quad x_2 > 0 . \tag{8}$$

Tab. 1. Coefficients of function g
Tab. 1. Współczynniki funkcji g

i	a_i^-	a_i^+
1	$2,5484639892834 \cdot 10^{-1}$	$5,354005768873343 \cdot 10^{-1}$
2	$-7,5967949432579 \cdot 10^{-2}$	$2,478875435258108 \cdot 10^{-1}$
3	$1,290788993123314 \cdot 10^{-1}$	$2,016835713871144$
4	$1,271609252756195$	$4,469844387253860 \cdot 10^{-1}$
5	$25,08717694766549$	$20,59405537372022$
6	$-6,2813551689544 \cdot 10^{-2}$	$-6,62$
7	$9,18$	$1,454448710668103 \cdot 10^{-1}$
8	$7,829080981244007 \cdot 10^{-3}$	$9,198608118171837 \cdot 10^{-2}$
9	$7,100659281016790 \cdot 10^{-3}$	$-2,04249100965408 \cdot 10^{-2}$
10	$2,141349009154247 \cdot 10^{-3}$	$1,580083444571437 \cdot 10^{-3}$
11	$2,153682576940481 \cdot 10^{-4}$	$1,46$
12	$-1,52$	

The coefficient $c = 2,99\,\text{rad}/\text{s}^2$ is identified from step responses of the system.

The coefficients a_i^- and a_i^+ are determined by the least-squares method. The results are given below.

3. Position Control

Position control is a common task for actuators with DC motors. The control goal is to set the output angle at a reference value and stop the rotation of the shaft. Two such control problems are stated. The first is a time-optimal problem of steering the system from the origin $x^0 = 0$ to a target state

$$x^f = \text{col}(x_1^f, x_2^f) , \quad x_1^f = \frac{10\pi}{9}\,\text{rad}, \quad x_2^f = 0 . \tag{9}$$

The second problem is to find a control that minimizes a quadratic performance index

$$S(u) = \frac{1}{2}\int_0^\infty \left(50\,(x_1 - x_1^f)^2 + x_2^2 + Ru^2 \right) \mathrm{d}t \tag{10}$$

on trajectories of the system with the initial state $x^0 = 0$ and x_1^f given by (9). The positive weighting coefficient R allows controlling the magnitude of u. We take $R = 240 \text{ rad}^2/\text{s}^2$, a certain compromise between control accuracy and cost.

3.1. Time-optimal and Suboptimal Control – Linear Model

We first review the time-optimal control law for the linear model (2), (3) and later propose a suboptimal, or near time-optimal control strategy. The admissible controls u are bounded (see (1)).

We will synthesize a time-optimal regulator that steers the system from an initial state x^0 to a target state x^f in minimum time. It can be easily verified that such a regulator exists and is unique. To construct it we shift the target state to zero by defining new state vector $z = \text{col}(z_1, z_2)$ with $z_1 = x_1 - x_1^f$, $z_2 = x_2 - x_2^f$. Putting this to equations (2), (3) we obtain the state equations in new coordinates

$$\dot{z}_1 = z_2$$
$$\dot{z}_2 = az_2 + bu \ .$$

The goal of time-optimal control changes to steering this system from an initial state $z^0 = x^0 - x^f$ to the origin.

As time-optimal controls in the considered system take only boundary values, we will need the families of state trajectories produced by constant controls equal to $+1$ and -1. Putting a constant u into the second state equation we obtain

$$z_2(t) = e^{at}z_2(0) - \frac{bu}{a}(1 - e^{at}) \ . \tag{11}$$

Since $\dot{z}_2 - a\dot{z}_1 = bu$, we have

$$z_2(t) - az_1(t) = but + z_2(0) - az_1(0) \ \text{ and}$$

$$z_1(t) = z_1(0) + \frac{1}{a}\big(z_2(t) - z_2(0) - but\big). \tag{12}$$

We distinguish two cases. If $az_2(0) + bu = 0$, then

$$z_1(t) = z_1(0) - \frac{b}{a}ut \ , \quad z_2(t) = -\frac{b}{a}u \ .$$

Let now $az_2(0) + bu \neq 0$. Formula (11) yields

$$t = \frac{1}{a}\ln\frac{az_2(t) + bu}{az_2(0) + bu} \ .$$

Substituting this expression in (12) we obtain the trajectory in the state space

$$z_1(t) = z_1(0) + \frac{z_2(t) - z_2(0)}{a} - \frac{bu}{a^2}\ln\frac{az_2(t) + bu}{az_2(0) + bu} \ . \tag{13}$$

The switching curve consists of two arcs. They are determined by (13) with the substitution $z_1(0) = z_2(0) = 0$. The first is obtained by putting $u = +1$ and selecting that part of the curve where $z_2 \leq 0$. The second arc is obtained by putting $u = -1$ and selecting that part of the curve where $z_2 \geq 0$. The switching curve has thus the form
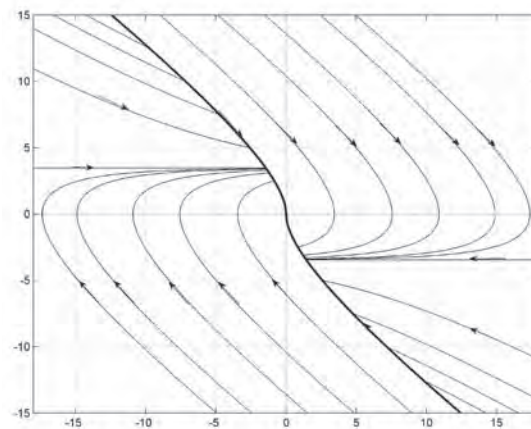

Fig. 3. Time-optimal state trajectories. The switching curve is drawn in bold line

Rys. 3. Czasooptymalne trajektorie. Krzywa przełączeń zaznaczona pogrubioną linią

$$z_1 = \varphi(z_2) \quad = \frac{1}{a}\begin{cases} z_2 - \dfrac{b}{a}\ln\left(1 + \dfrac{a}{b}z_2\right), & z_2 \leq 0 \\[3mm] z_2 + \dfrac{b}{a}\ln\left(1 - \dfrac{a}{b}z_2\right), & z_2 \geq 0. \end{cases}$$

The time-optimal regulator is given by (see Figure 3)

$$u = \rho(z) = \begin{cases} -1, & z_1 > \varphi(z_2) \ \text{or} \ z_1 = \varphi(z_2) \ \text{and} \ z_2 < 0 \\ 0, & z = 0 \\ +1, & z_1 < \varphi(z_2) \ \text{or} \ z_1 = \varphi(z_2) \ \text{and} \ z_2 > 0. \end{cases} \tag{14}$$

For $x^0 = 0$ and x^f given by (9), the time-optimal control has one switching at $t_1 = 1{,}6$ s and the optimal horizon is $T = 2{,}34$ s.

The time-optimal control is very sensitive to parameter variations. Therefore the model coefficients should be properly identified. It is a well known effect that the time-optimal rule (14) results in chattering of the servomechanism due to measuring noise. Near the origin the motor is excited by a control sequence: $+1, -1, +1...$ switched with a high frequency. To avoid such effects one can change the time-optimal algorithm in a neighborhood of the origin. For example, a decaying factor can reduce the amplitude of control.

The time-suboptimal control algorithm that reduces the chattering of the system works according to (14), but with the control bounds modified in a neighborhood of the target. In the beginning $u_{max} = 1$ (as in (1)). In each time step it is checked if $|z_1| < M$, for some predetermined $M > 0$. If so, the bound for u is decreased, $u_{max} := \dfrac{|z_1|}{M}u_{max}$. Otherwise, $u_{max} := 1$.

3.2. Time-optimal Control – Nonlinear Model

The nonlinear model of DC motor is given by (4) and (5), with the function $g(x_2)$ determined by (6)–(8). The control u satisfies (1). To remove the discontinuity of $g(x_2)$ at zero we multiply it by an arctan function. The state equations take the form

$$\dot{x}_1 = x_2 \tag{15}$$

$$\dot{x}_2 = c\left(u - \tfrac{2}{\pi}g(x_2)\left|\arctan(\alpha x_2)\right|\right) \tag{16}$$

where $\alpha = 1000$. The adjoint equations read

$$\dot{\psi}_1 = 0$$

$$\dot{\psi}_2 = -\psi_1 + \frac{2}{\pi} c\psi_2 \left(\frac{\alpha g(x_2)}{1 + \alpha^2 x_2^2} + \arctan(\alpha x_2) \nabla g(x_2) \right) \mathrm{sgn} x_2$$

The time-optimal control has a bang-bang character, $u(t) = \mathrm{sgn}\,\psi_2(t)$. The optimal solution is computed with the use of the MSE method described in [2–4]. The optimal horizon is $T = 2{,}2713$ s and the optimal control has one switching at $t_1 = 1{,}596$ s.

3.3. Time-optimal Control Experiments

In the investigated system the sample time cannot be less than 0,01 s due to the applied technology. For this reason in real-time experiments the switching time t_1 is set to 1,6 s and the accuracy of measurement of the horizon T is 0,01 s.

Two experiments are performed and compared. In the first experiment, the time-optimal control calculated for the
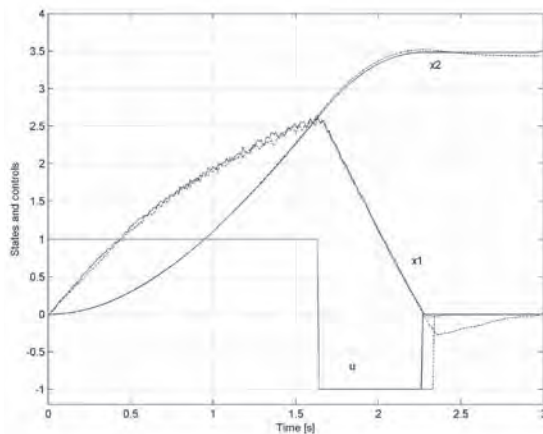

Fig. 4. "Improved" time-optimal trajectories and controls (dashed lines – linear model, solid lines – nonlinear model)

Rys. 4. "Poprawione" trajektorie czasooptymalne i sterowania (linie przerywane – model liniowy, linie ciągłe – model nieliniowy)
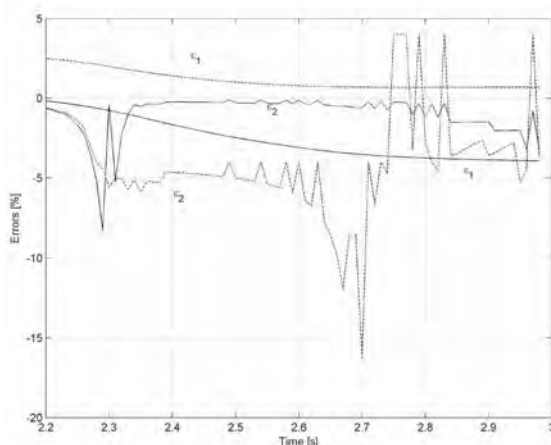

Fig. 5. Errors of real-time experiments in comparison to simulation results (dashed lines – linear model, solid line – nonlinear model)

Rys. 5. Porównanie eksperymentów w czasie rzeczywistym z wynikami symulacji (linie przerywane – model liniowy, linie ciągłe – model nieliniowy)

linear model is used, with the horizon $T = 2{,}34$ s and one switching time $t_1 = 1{,}6$ s. In the second, the time-optimal control computed for the nonlinear model is applied. As the switching time is the same as in the linear case, the only difference is that the control is switched off and the result assessed earlier, at the optimal horizon $T = 2{,}27$ s. It appears that the angular velocity of the DC motor is not equal to zero at the corresponding times T in both cases. This means that the switching time is a little too small, and in consequence the angle does not reach the target value.

To correct the errors we increase the switching time to 1,62 s and repeat the experiments. The horizons are not changed. Fig. 4 presents the responses of the real DC motor after improving the switching time. Note that the angle and velocity errors are less at the horizon optimal according to the nonlinear model. The relative angle error is then equal to –1,31 % whereas it is –2,91 % at the optimal horizon calculated for the linear model. The responses presented in Fig. 4 are undistinguishable up to 2,27 s.

From this time onward they differ because the controls are switched off (set to zero) at the corresponding, different optimal horizon times. A comparison of the presented experiments and simulation results obtained with the use of the nonlinear model and the modified time-optimal control is given in Fig. 5 where the errors for time greater than 2,2 s are plotted. The position error is denoted by ε_1 and the velocity error by ε_2. Each curve represents the difference between the simulated and real-time trajectories obtained for the same, modified time-optimal control.

3.4. Comparison of Time-optimal and Suboptimal Solutions

The time-suboptimal algorithm previously described has been applied in a real-time experiment. The control is bounded according to (1) and the parameter $M = 0{,}1$ rad. The initial state $x^0 = 0$ and the target state x^f is given by (9).

The comparison of the time-optimal control for the nonlinear model and the time-suboptimal control is shown in Fig. 6. The steady state error of x_1 is 0,4 % if the optimal control is
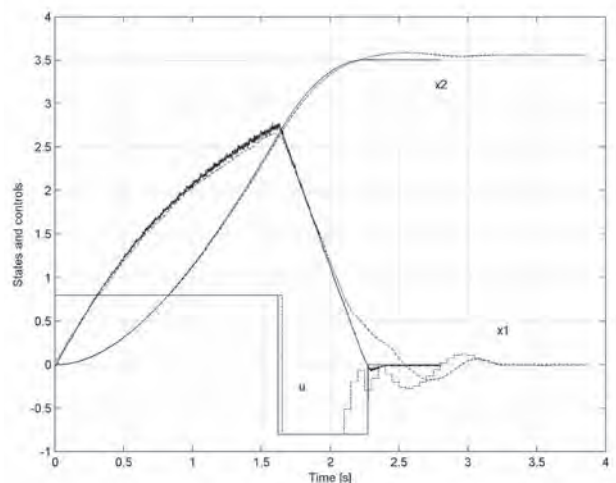

Fig. 6. Time-suboptimal (dashed lines) and time-optimal trajectories and control (solid lines)

Rys. 6. Suboptymalne (linie przerywane) i czasooptymalne trajektorie i sterowania (linie ciągłe)

applied, and 4% in the case of suboptimal control. The control time is 2,27 s in the first case and 3,25 s in the second.

Note that the nonlinear model used to calculate the optimal control is not precisely identified. In our very simple approach, the model contains only the nonlinearity of static characteristic. Despite it the optimal control obtained with the aid of the nonlinear model is much better than the suboptimal one, calculated according to the linear model.

3.5. Quadratic-optimal and Suboptimal Control

Position control, suboptimal and optimal in the sense of the quadratic performance index (10) is considered in this section. First, we use the linear model (2), (3) of the DC motor to design an LQ-optimal controller. The control bounds are neglected in the calculations. The solution of the LQ problem with the initial state $x^0 = 0$ and x_1^f (9) yields the controller gain matrix $K = [0,4564 \ 0,3569]$. The suboptimal controller used in the experiment has the form

$$u_{l_q}(t) = -\begin{cases} Kz(t), & |Kz(t)| \le 1 \\ \operatorname{sgn}(Kz(t)), & |Kz(t)| > 1. \end{cases}$$
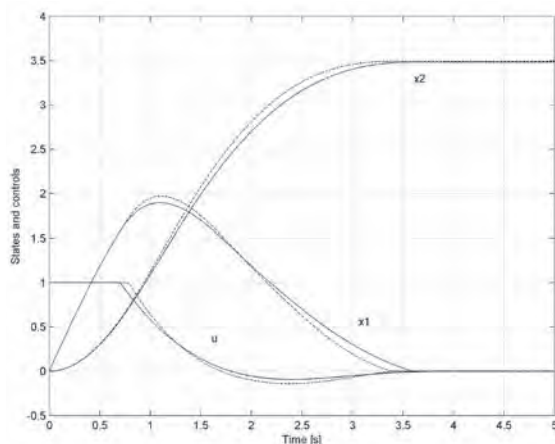

Fig. 7. Comparison of simulation experiments: suboptimal (dashed lines) and optimal (solid lines) trajectories and control

Rys. 7. Porównanie eksperymentów symulacyjnych: suboptymalne (linie przerywane) i optymalne (linie ciągłe) trajektorie i sterowania
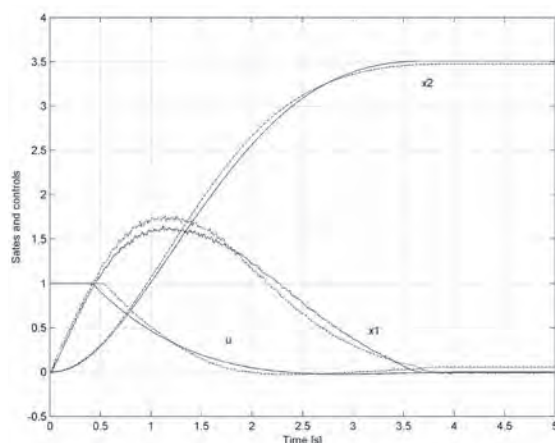

Fig. 8. Comparison of real-time experiments: suboptimal (dashed lines) and optimal (solid lines) trajectories and control

Rys. 8. Porównanie eksperymentów w czasie rzeczywistym: suboptymalne (linie przerywane) i optymalne (linie ciągłe) trajektorie i sterowania

Note that this controller is not optimal with respect to the performance index (10). The corresponding value of this index is $S_{l_q} = 13341{,}2$. Next, an optimal control u_{opt} is calculated for the nonlinear model (15), (16) with the control bounds (1) taken into consideration. In this case the Hamiltonian has a form

$$H = \psi_1 x_2 + \psi_2 c \left(u - g(x_2) \right) - 25\left(x_1 - x_1^f\right)^2 - \tfrac{1}{2}\left(x_2^2 + Ru^2\right)$$

and the adjoint equations read

$$\dot{\psi}_1 = 50\left(x_1 - x_1^f\right)$$

$$\dot{\psi}_2 = -\psi_1 + \tfrac{2}{\pi} c\psi_2 \left(\frac{\alpha g(x_2)}{1 + \alpha^2 x_2^2} + \arctan(\alpha x_2)\nabla g(x_2) \right)\operatorname{sgn} x_2 + x_2$$

The optimal control maximizes the Hamiltonian and satisfies

$$u(t) = \begin{cases} \dfrac{c}{R}\psi_2(t), & \dfrac{c}{R}|\psi_2(t)| \le 1 \\ \operatorname{sgn}\psi_2(t), & \text{otherwise.} \end{cases}$$

The optimal solution is computed with the use of the MSE method described in [2, 3]. The optimal value of the performance index is $S_{opt} = 12465{,}24$. Figures 7, 8 present the results of simulation and real-time experiments, respectively. In both figures a comparison of the controls u_{l_q} and u_{opt} is shown. Solid lines are related to the optimal control and dashed lines to the suboptimal control.

4. Conclusions

Position control of DC motor is discussed and two control problems are investigated: first, time optimal and second, optimal in the sense of a quadratic performance index. Simple mathematical models, linear and nonlinear, of the DC motor are introduced. In the presented approach, the nonlinear model contains only the nonlinearity of static characteristic. Controllers based on linear and nonlinear models are constructed for both control problems. For the nonlinear model optimal solutions are computed with the use of the MSE method. The experimental results show that the optimal controls obtained with the aid of the nonlinear model, even not very accurate, give better results than calculated according to the linear model.

References

1. Kuo B.: *Automatic Control Systems*. Englewood Cliffs, NJ: Prentice Hall 1995.
2. Szymkat M., Korytowski A., Turnau A.: *Extended variable parameterization method for optimal control*. Proc. 2002 IEEE Int. Symp. Comp. Aid. Contr. Syst. Des., Glasgow, Scotland, UK, 2002.
3. Szymkat M., Korytowski A.: *Evolution of structure for direct control optimization*. Discussiones Mathematicae Differential Inclusions, Control and Optimization 27, 2007.
4. Szymkat M., Korytowski A.: *Method of monotone structural evolution for control and state constrained optimal*

control problems. Proc. European Control Conference ECC 2003, Univ. Cambridge, UK, 1-4 Sept., 2003.

5. *MATLAB 6.5.1.* The MathWorks, Inc., Natick, USA, 2003. ■

Optymalne sterowanie laboratoryjnym serwomechanizmem z silnikiem prądu stałego

Streszczenie: W pracy przedyskutowano dwa problemy sterowania pozycyjnego serwomechanizmem z silnikiem prądu stałego: problem czasooptymalny oraz sterowanie optymalne w sensie kwadratowego wskaźnika jakości. Przedstawiono proste modele matematyczne: liniowy i nieliniowy. W nieliniowym modelu uwzględniono jedynie nieliniową charakterystykę statyczną silnika. Dla obydwu problemów zaprojektowano regulatory wykorzystując modele liniowy i nieliniowy. Optymalne sterowanie dla modelu nieliniowego obliczono za pomocą metody MSE. Przedstawiono porównanie eksperymentów symulacyjnych i eksperymentów czasu rzeczywistego.

Słowa kluczowe: sterowanie optymalne, serwomechanizm, metoda MSE, sterowanie czasooptymalne

Krystyn Hajduk, PhD

He received MSc in Electronics and Telecommunication and PhD in Automatics both from the Faculty of Electrical Engineering, Automatics, Computer Science and Electronics, AGH University of Science and Technology in Cracow, Poland. Currently he works as assistant professor at Department of Automatics AGH. His research areas concern control theory including implementation of real-time control algorithms, rapid prototyping and intelligent control systems.

e-mail: kha@agh.edu.pl

Przemysław Gorczyca, PhD

He works at Department of Process Control, AGH University of Science and Technology since 1970 year. Received his MSc in Electrical Engineering in 1970 and PhD degree in Modelling of Industrial Process in 1975 both from the Faculty of Electrical Engineering, Automatics and Electronics (present: Faculty of Electrical Engineering, Automatics, Computer Science and Electronics, EAIiE), AGH University of Science and Technology in Cracow, Poland. He specialises in identification and modelling of industrial processes. He is the author and co-author of many papers published in journals and proceedings of scientific meetings.

e-mail: przemgor@agh.edu.pl

Krzysztof Kołek, PhD

Received his MSc in Electrical Engineering in 1989 and PhD degree in Real-Time Systems Control in 1996 both from the Faculty of Electrical Engineering, Automatics and Electronics (present: Faculty of Electrical Engineering, Automatics, Computer Science and Electronics, EAIiE), AGH University of Science and Technology in Cracow, Poland. In 1989 he joined the academic staff of the Institute of Automatics at the AGH University of Science and Technology, where he works currently as an assistant. His research activities are primarily devoted to real-time control design, practical applications of real-time strategies and applications of reconfigurable digital circuits in automatic control systems. He is the author and co-author of over 50 papers published in journals and proceedings of scientific meetings.

e-mail: kko@agh.edu.pl